Implementation and performance evaluation of a real time pulse blanker for RFI mitigation in radio astronomy

A. Tani[1,2], G. Comoretto[1]

[1]Osservatorio Astrofisico di Arcetri
[2] Università degli Studi di Firenze

Arcetri Technical Report N° 9/2011
Firenze, Dicembre 2011

Abstract

Impulsive Radio frequency Interference (RFI) could be a serious threat for observations in the radio astronomy bands, particularly for L-band spectroscopy. This report is focused on the implementation of a real time mitigation strategy based on temporal blanking. Furthermore, the implementation of a real time peak detector to identify the impulsive RFI is also discussed. Finally, to highlight the robustness of the proposed detector, its performance in term of detection probability and false alarm probability is reported under different operating conditions both theoretically and by simulations using a test signal generator.

1 Introduction

The increased sensitivity of the next generation radio telescope makes them more vulnerable to radio unwanted emissions (Radio frequency Interference, RFI), caused by the increased spectrum utilization due to the Telecommunication systems and Radars.

In particular, the pulsed RFI from the ground-based aviation radar can severely affect spectroscopy at L-band and also pulsar observation. The radar effect on the receiver is twofold: first the information at the radar frequency is completely lost, second if the radar pulse is sufficiently strong it can cause distortion due the receiver response saturation.

Regulation can protect particular windows of the radio spectrum but many observations need to access to a wider spectral range which can be still contaminated by such broadband interference. In the literature, several signal processing strategies providing pulsed RFI mitigation, based on temporal blanking or cancellation have been presented [1][2].

The aim of this report is the description and the implementation of a pulse-blanking algorithm that is capable of removing reliably pulsed time-domain interference sources in real time. Furthermore, we focused on the detection algorithm which triggers the blanking, and the performance in term of false alarm probability and detection probability by means of FPGA simulations is derived

The report is structured as follows: in the first section, after a brief introduction on the overall system, the proposed RFI detection algorithm is described. In the second section we illustrate how the blanker works, using a state diagram and the hardware resources employed in the FPGA implementation are also discussed. Finally after a brief description of the simulation environment and of the parameters used, the performance results and the data loss are presented.

2 The Pulse Blanker System

2.1 Introduction

Generally for receivers operating at a sufficiently high sampling frequency, an efficient strategy for mitigating pulsed RFI is to remove (or blank) incoming data whose power exceeds a predefined threshold function of the mean power.

The detector generates a *trigger signal* to activate the blanker. However, because the detection time is not zero, i.e. the RFI pulse starts before the detection process is completed, we have to blank all data eventually corrupted before the trigger signal (*pre-detection blanking)*, hence a buffer is required. The buffer length determines the maximum *pre-detection* time. Then, in order to ensure that any pre and post-detection data corrupted by the pulse is successfully removed, after flushing the buffer, the trigger sets the output to zero for a proper period (*post-detection period*).

A block scheme of the detector and mitigator is depicted in Fig. 1. Clearly, when the trigger signal is low, the output is simply a time shifted version of the input.

2.2 The Detection Algorithm

A brief overview of the RFI detection basic concepts will be presented here. In general, the signal received from a single dish antenna, $r(t)$ can be written as:

$$r(t) = n(t) + s(t) \tag{1}$$

where $n(t)$ is the Additive White Gaussian Noise (AWGN) which includes the receiver noise, sky noise and the radio astronomical source, while $x(t)$ takes into account the RFI. The RFI detection is a classical statistical signal processing problem and it can be formulated as the following, well known, *hypothesis testing*:

$$\begin{cases} \mathrm{H}_0 : r(t) = n(t) \\ \mathrm{H}_1 : r(t) = s(t) + n(t) \end{cases} \tag{2}$$

where H_0 is the *null hypothesis* (i.e.,the absence of the interference), and H_1 is the *alternative hypothesis* (i.e., the presence of the interference). The hypothesis testing is a statistical test which

discriminates between the hypothesis H_0 and H_1. In particular, the statistical test is a random variable obtained by a set of samples of the received signal.

As a consequence, to evaluate the performance of an RFI detector, we define the RFI detection probability P_d, as the probability that the statistical test gives a correct decision when H_1 is true. On the other hand, we denotes with P_{fa} the false alarm probability, i.e., the probability that the statistical test gives a wrong decision under the hypothesis H_0.

As depicted in Fig. 1, the proposed detector relies on signal power estimation. In general, the power of a discrete time signal $s(i)$ can be expressed as follows:

$$\sigma_s^2 = \lim_{N\to\infty} \frac{1}{N} \sum_{i=0}^{N-1} s(i)^2 = R_{ss}(0) \tag{3}$$

where $R_{ss}(0)$ is the autocorrelation of $s(i)$ evaluated at lag zero and N is the number of samples used for the estimation. Recalling that the autocorrelation R_{ss} of a discrete time signal $s(i)$ is defined as:

$$R_{ss}(i) = \lim_{N\to\infty} \frac{1}{N} \sum_{n=0}^{N-1} s(n)s(n-i) \tag{4}$$

then denoted with $\hat{R}_{ss}(0)$, the estimation of the autocorrelation, the estimation computed in Fig. 1 results to be:

$$\hat{\sigma}_s^2 = \frac{1}{N} \sum_{i=0}^{N-1} s(i)^2 = \hat{R}_{ss}(0) \tag{5}$$

It can be shown that this estimator is unbiased and consistent, because it converges to the true value for $N \to \infty$. Denoting with $\hat{\sigma}^2_{peak}$ the peak power estimation and with $\hat{\sigma}^2_{mean}$ the mean power estimation, the Test Statistic T used to reveal the impulsive RFI, can be expressed as follows:

$$T = \frac{\hat{\sigma}^2_{peak}}{\hat{\sigma}^2_{mean}} \gtrless T_h \tag{6}$$

where T_h is a proper threshold. The P_{fa} depends on T_h and N.

As depicted in Fig. 1, the proposed detector works as follows: the input signal $s(t)$ is squared and then in the upper branch the squared signal is integrated for a time T_1 to produce an estimation of the mean power of the signal, ($\hat{\sigma}^2_{mean}$). The integrator is implemented as a moving average (or *boxcar*), so that its value is updated every clock cycle. In the lower branch the input signal is squared and then integrated for a time $T_2 \simeq \tau \ll T_1$, where τ stands for the impulse duration, providing a peak power estimation ($\hat{\sigma}^2_{peak}$). Finally the signals originated by the two branches are compared and if the signal of the lower branch exceeds the upper one by the factor T_h, the comparator generates a trigger that blanks the signal.

Ideally for $N \to \infty$, both $\hat{\sigma}^2_{peak}$ and $\hat{\sigma}^2_{mean}$ converge to their real values. Hence, under the H_0 Hypothesis $T \to 1$, and $P_{fa} \to 0$, $\forall\, T_h > 1$

The target P_{fa} and P_d are respectively 0 and 1. However, due to the *noise uncertainty*, i.e., to the availability of a reduced observation time, the P_{fa} and P_d targets can be reached only for high value of Interference to Noise Ratio (INR) and T_h

It is interesting to note that, because the impulse duration τ is known, the (2.2) implemented in the lower branch can be considered the impulsive interference autocorrelation evaluated at lag zero (under the H_1 hypothesis).

This consideration could lead to implement a different detector based on the Matched Filter concept, if also the shape of interference impulse is known.

2.3 State Diagram

The state diagram reported in Fig. 2 describes how the blanker works. The buffer is implemented as a First In First Out data structure (FIFO), hence in the diagram it is denoted as FIFO.

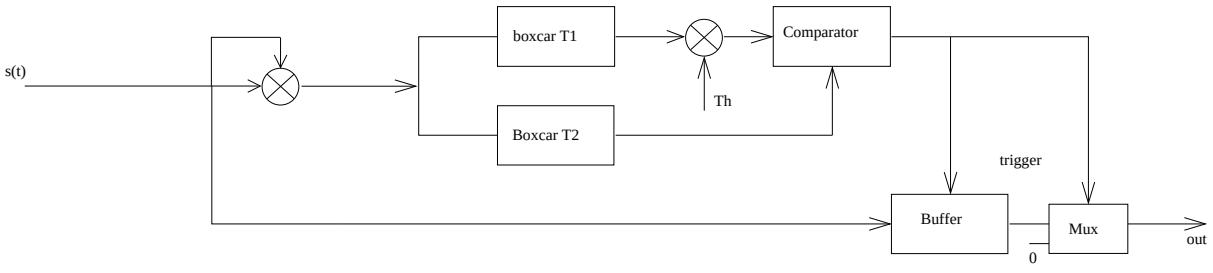

Figure 1: System Block Scheme

The first operation is the FIFO initialization: during this phase the FIFO is filled with the incoming samples and the output is set to zero.

Assuming the H_0 hypothesis, when the FIFO becomes full it is read once, then the normal_mode flag is set to 1 and the system goes to *the normal_mode state*. In this state, both reading and writing the FIFO are allowed and the output of the system is the output of the FIFO . Therefore in this case the output is a replica of the input shifted in time by an amount equal to buffer dimension.

When the trigger becomes high (i.e., an interference is detected) the FIFO is flushed, the FIFO EMPTY state is reached, the normal_mode flag is set to zero and the counter of the *post-detection* starts. When the count is finished, the *post-detection* phase is terminated, and if the trigger is zero, the FIFO is initialized again. Otherwise, it means that the interference is still present and the system remains in the FIFO EMPTY state, and the counter is reset. In this way the blanker can also mitigate interferences longer than 6.4μs.

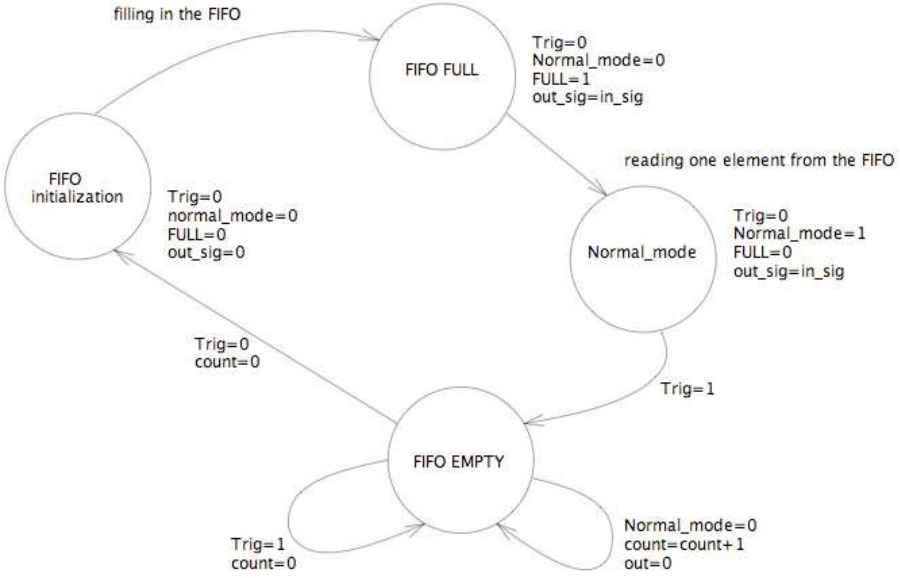

Figure 2: State diagram

2.4 Hardware Implementation

The resources employed in the FPGA implementation are described in the table 1. The buffer is implemented as a SCFIFO (Single Clock FIFO) a component of Altera Megawizard, (for details about

the signals used in this component see [4]). The boxcar module has been implemented with a shift-register (likewise a FIFO data structure) of unsigned 24 bits using the *loop* construction. In order to save hardware resources the integration is computed as follows: at each clock cycle, the FIFO top element is added to the accumulator, while the bottom one is subtracted.

The table 1 highlights the limited hardware resources used for the FPGA implementation.

Modulo	logic cells	LC Registers	Memory bits	DSP Elements	DSP 18x18
Radar_blanker (Total)	1058 (290)	805	27072	2	1
FIFO	58 (0)	36	3072	0	0
RFI_detect1 (Total Detection)	710 (137)	577	24000	2	1
boxcar_long_term	355 (345)	306	24000	0	0
boxcar_short_term	180 (180)	134	0	0	0
comparator	38 (38)	0	0	0	0
mult 23	0	0	0	2	1

Table 1: Resources employed for the algorithm

3 Simulation

3.1 Signal model and Simulation Parameters

The simulation has been carried out feeding the system with a test signal generated within the FPGA by a VHDL module termed *pulse_shaper*. The test signal models the impulsive noise with a *Gated Gaussian Noise*. In order to generate this signal, first, an approximated Gaussian noise has been generated summing five pseudo-random signals obtained with a Linear Feedback Shift Register (LFSR). Then the *pulse_shaper* acts as a gating function to filter the Gaussian noise with a rectangular ideal filter.

The parameters of the test signal, using the radar terminology, are: Pulse Repetition Period and Pulse width; obviously this parameters can be varied to simulate different situations (i.e., different radar pulses).

The clock signal used is the Altera's FPGA internal clock that provides a sampling time of 0.0125μs (80 MHz). As a consequence the simulated pulsed interference has a duration of 1.6 μs, the *pre-detection* time (equal to the buffer dimension) is 3.2μs, while the *post-detection* time is equal to the *pre-detection* one, so that the overall blank-time is 6.4μs. The pulse amplitude ranges from 1 to 0.125 of the noise amplitude, and hence the INR varies from 0 to -9 dB The paramaters used in the simulation are summarized in the table below:

Parameters	samples	time
Clock Period	-	0.0125μs
FIFO depth	256	3.2 μs
Boxcar 1 (long) duration	128	1.6 μs
Boxcar 2 (short) duration	1024	12.8 μs
Pulse duration	128	1.6 μs
Pulse Repetition Interval	1408	17.6 μs
Overall Blanking Time	512	6.4 μs

Table 2: Parameters used in the performance evaluation, expressed in samples and time

3.2 Simulation Results

As described before, the modules related to the test signal generation (*Gaussian Noise* and *Pulse Shaper*) have been embedded in the VHDL top level design which includes as DUT (Device Under Test) both the detection algorithm and the blanker. In order to evaluate the performance of an RFI detector we have to compute the RFI detection probability, P_d, and the the false alarm probability P_{fa}. For this purpose, the top level includes two counters: *out_H1*, which takes into account of the number of correct detections and *out_frame_number*, which is the counter related to the number of tests performed. The ratio *out_H1/out_frame_number* gives an approximation of P_d under the H_1 hypothesis while it gives an approximation of P_{fa}, under the H_0 hypothesis.

The Fig. 3 is a screen-shot taken from Quartus Signal Tap logical analyzer and it highlights the most important signals used in the simulation, in particular the first two rows represent the two counters above described: the *out_frame_num* and the counter *out_H1*.

The signal *out_pulse_gen* is the test signal, i.e., the *Gated Gaussian Noise*, input of the blanker system. In the case depicted in the Fig. 3, the INR=0, i.e., the interference has the same amplitude of the noise and three impulses, with the same duration equal to 128 samples and spaced by 1408 samples, can be easily noted.

The signals *out_mean_pow* and *out_peak_pow* illustrate how the detector works. The signal *out_mean_pow* is the result of the integration of the test signal a with a *boxcar integrator* (or moving average) of width equal to 1024 samples. This integration yields an approximation of mean power of the incoming signal and it is therefore approximatively constant in time, as depicted in Fig. 3.

On the other hand the signal *out_peak_pow* represents the output of a boxcar whose window is 128 samples and it provides an estimation of the peak power of the incoming signal. As stated in the previous section, this signal represents also the time varying autocorrelation function computed at lag zero. As a consequence, when the impulse arrives, the *out_peak_pow* exhibits the triangular shape typical of the autocorrelation of a rectangular impulse, clearly visible in the Fig. 3 and whose peak represents the estimated power of the impulse.

When the ratio between *out_peak_pow* and *out_mean_pow* exceeds a previously chosen threshold, the *out_trig* becomes high and it activates the blanker (*trigger signal*). In this case the trigger remains high for exactly 256 samples, due to the perfect detection of an impulse whose duration is 128 samples.

It is important to note that an impulse larger than 128 samples would produce an *out_trig* larger than 256 samples, hence enabling the blanker for 256 samples more, because if the post detection counter is reset when the trigger is still high we have a new run of the post detection counter.

The signal *out_sig* is the output of the blanker and it is zero, wherever the trigger is high, otherwise the output is a replica of the input signal shifted in time by an amount equal to the buffer detector dimension. In the case depicted in the Fig. 3, the gaps (512 samples long) in the *out_sig* highlight the activation of the blanker.

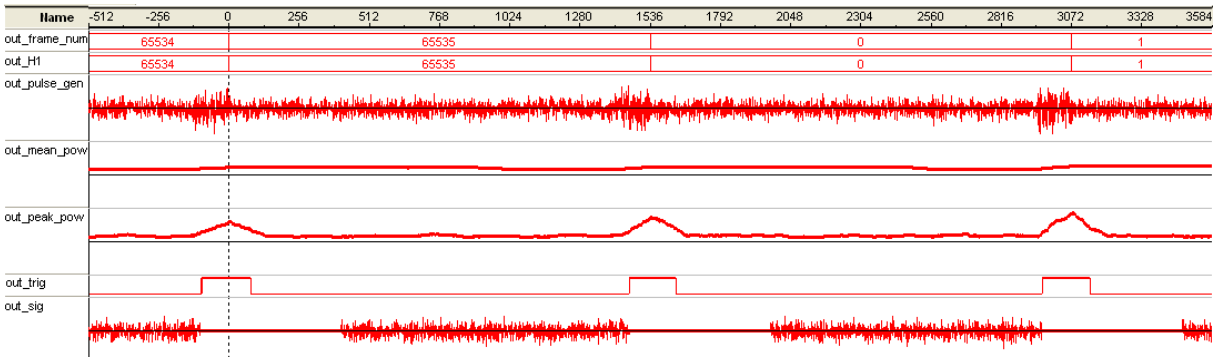

Figure 3: Quartus Signal Tap logical Analyzer screenshot, INR=0 dB, Th=1.5, 4K samples

3.2.1 Simulation Scenarios

In this section,we discuss the typical simulation scenarios encountered by our detector in the hypothesis testing under different INR conditions and for various threshold values.

Firstly, we assume that the H_0 hypothesis is true, in this context, the Fig. 4 illustrates a False Alarm case (also termed Wrong Decision Type I), i.e., we reject the H_0 hypothesis, assessing the presence of the interference in the incoming signal. In this case, the *out_peak_pow* and *out_mean_pow* signals are very close and the threshold T_h set to 1.125 can not guarantee a sufficient P_{fa} (~ 0.1).

On the other hand, the Fig. 5 highlights that the system correctly assess the absence of interference when H_0 Hypothesis is true, using a threshold T_h=1.25 (P_{fa}=0.013) higher than that used in case depicted in the Fig. 4.

Now, assuming that the H_1 hypothesis is true, Fig. 6 and Fig. 7 illustrate the correct decision with $T_h = 1.125$ in the high INR (INR=0 dB) and low INR (INR =-9 dB) case, respectively.

Finally the Fig. 8 illustrates a Wrong decision (Type Error II) in the Low INR case (INR= -9dB), using a $T_h = 1.125$

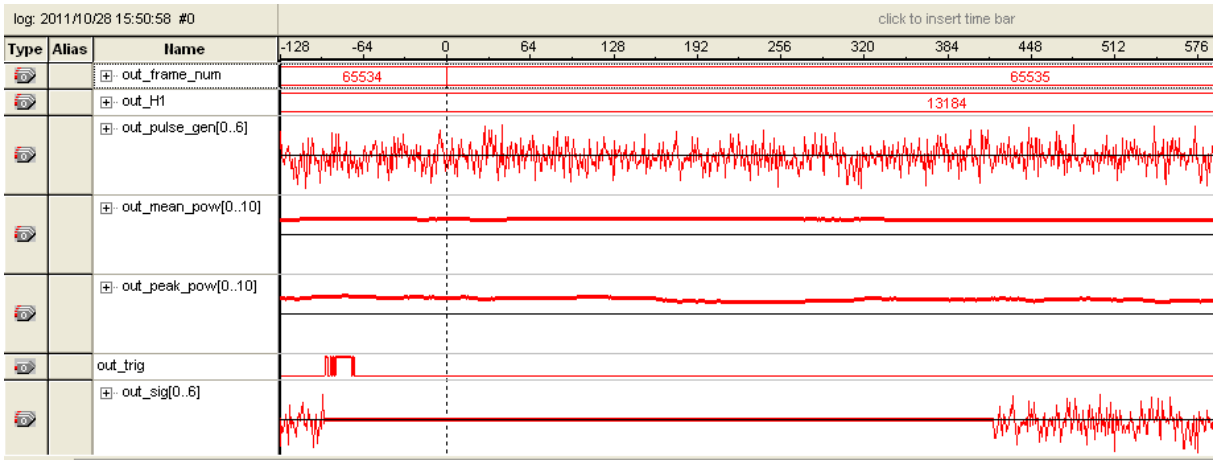

Figure 4: Quartus STLA screenshot 2 : (False Alarm case) Wrong decision under H_0 Hypothesis , Th=1.125 (P_{fa}=0.1)

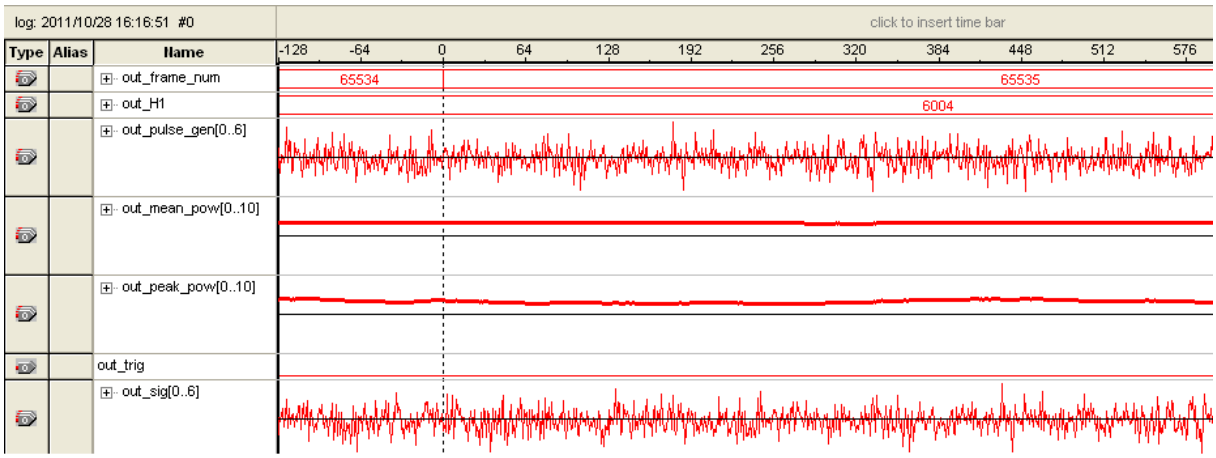

Figure 5: Quartus STLA screenshot 3 : Right Decision under H_0 Hypothesis, Th=1.25 (P_{fa}=0.013)

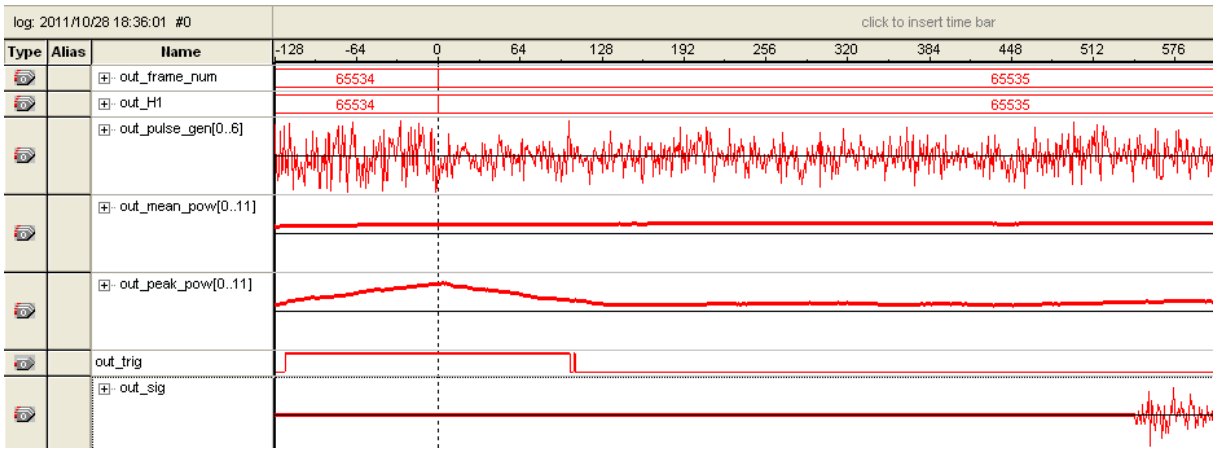

Figure 6: Quartus STLA screenshot 7 : Right Decision with high INR, under H_1 Hypothesis, INR=0 dB, Th=1.125 (P_{fa}=0.1)

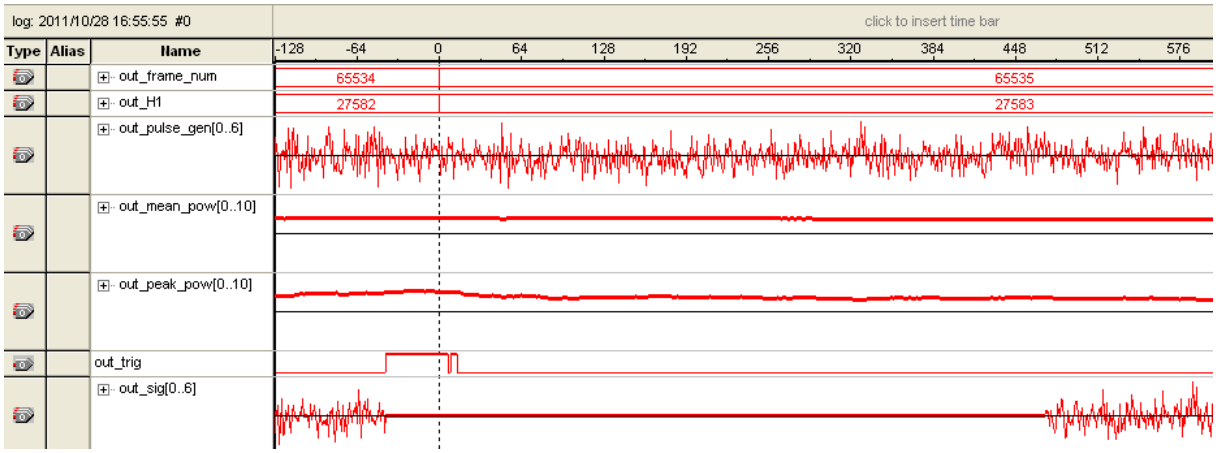

Figure 7: Quartus STLA screenshot 5 : Right Decision with low INR, under H_1 Hypothesis INR= -9dB, Th=1.125 (P_{fa}=0.1)

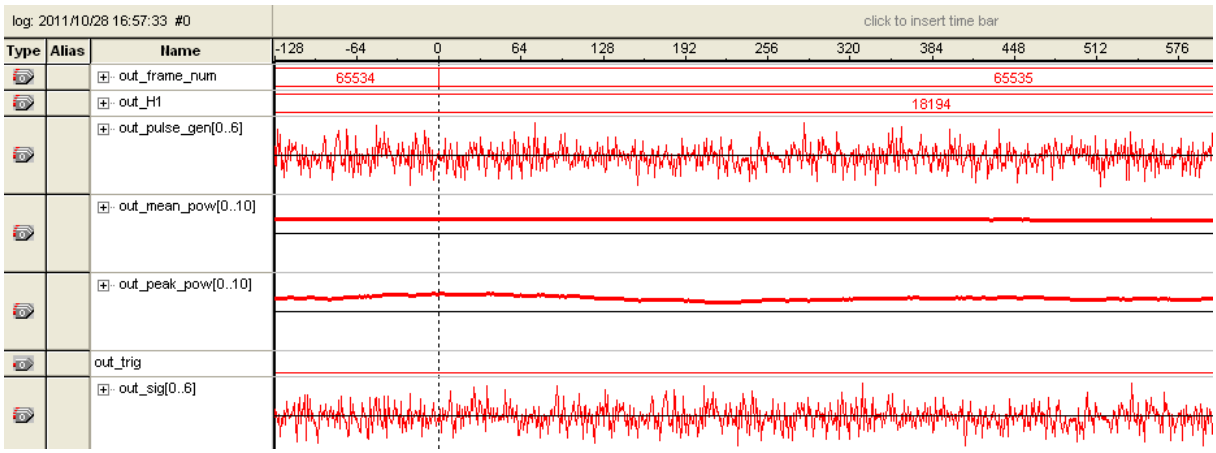

Figure 8: Quartus STLA screenshot 6 : Wrong Decision with low INR under H_1 Hypothesis, INR= -9dB, Th=1.125 (P_{fa}=0.1)

3.2.2 Detection Performance and data loss

In this section, the most important results concerning the detection algorithm are illustrated. In particular, Fig. 9 shows the performance of our method in terms of detection probability P_d as a function of the INR, for three different values of P_{fa}. In particular, Fig. 9 shows that the P_d increases as the INR increases for a given P_{fa}, while the P_d rises as the P_{fa} increases for a fixed INR.

This result can be compared to the that one presented in [3], where an approach based on χ^2 distribution model is employed to detect Radar pulses. In particular, the blue curve in Fig. 9 (related to a P_{fa} of $3{\cdot}10^{-5}$) has been compared with the curve WP (Weak Pulses) plotted for a P_{fa} of $1.3 \cdot 10^{-5}$ reported in [3]. Our detection method can detect pulses 3 dB weaker than that revealed with the method proposed in [3].

Generally it is assumed a target Detection Probability near to 1, and the corresponding False Alarm Probability for a given INR can be related to the *data loss*. For instance, for an INR of -4 dB, the data loss is about 0.012. In other words, for each second of data, 12 ms di data are lost. Therefore if a lower data loss is required, this implies an higher INR, i.e., an higher minimum detectable interference with a constraint of P_d=1.

According to the ITU-R recommendation 1513 [5], allowed data loss in the allocated RAS bands amount to 2% for single systems and 5% for aggregate systems. Generally the 2% of data loss is accepted as practical limit. In our simulation the P_{fa} considered is always less than 1%.

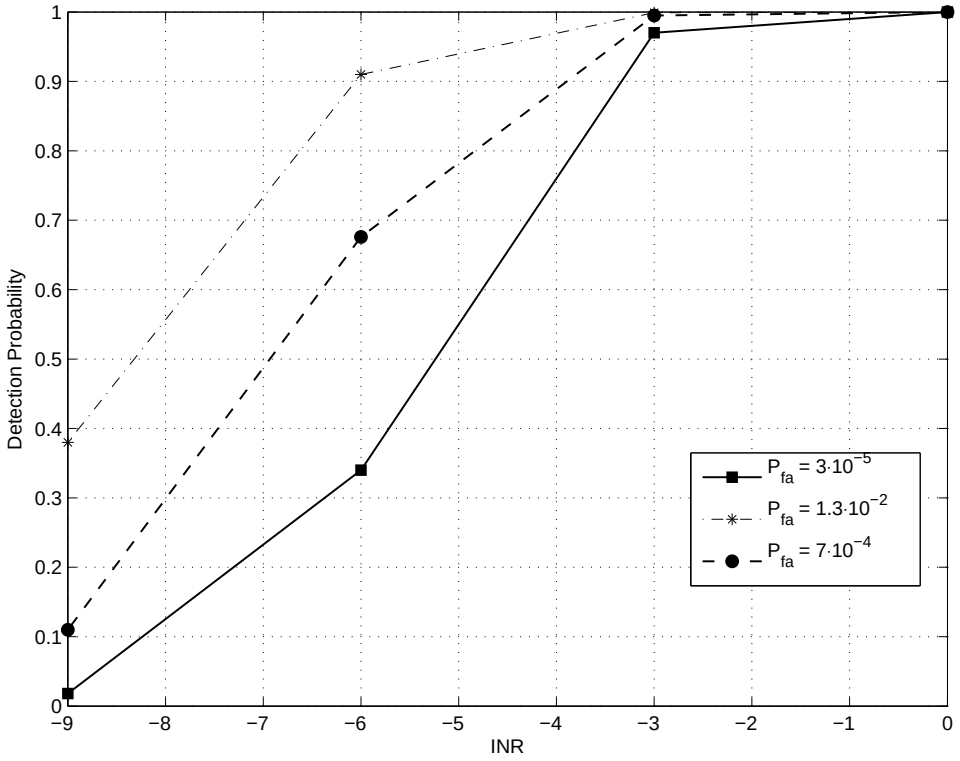

Figure 9: Detection Probability versus INR for different False Alarm Probabilities

Fig. 10 shows the Receiver Operating Characteristic (ROC) curves, i.e., P_d as function of the P_{fa} for different INR values. As the INR increases the curve approaches the optimal characteristic, in other words the detector exhibits a P_d close to 1, regardless of the P_{fa}. Therefore our detector has optimal characteristic for an INR not lower than -3 dB, but it exhibits good performances still up to -6 dB.

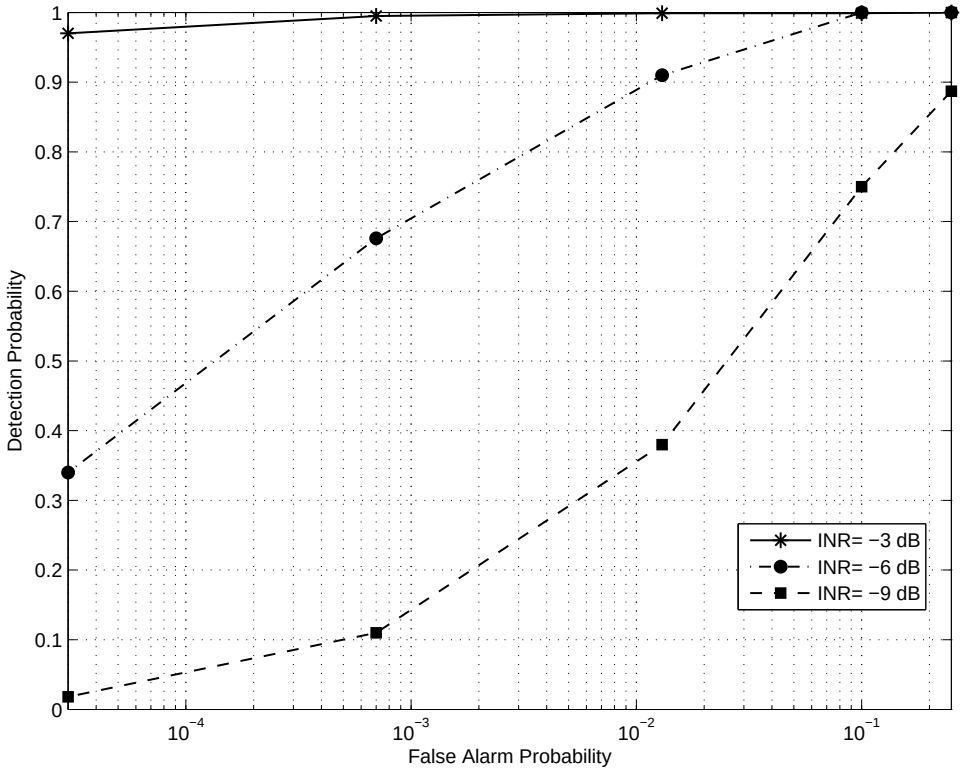

Figure 10: ROC curves for different INR

4 Conclusions

In this report the FPGA implementation of a real time method for impulsive RFI detection and mitigation has been described.

In particular, the mitigation relies on the temporal blanking of data corrupted by the RFI, revealed by a peak detector, which is based on the comparison between the peak power and estimated mean power.

Performance analysis in term of ROC curves and in terms of Detection Probability of RFI vs INR are derived, by means of FPGA simulations, to validate our method capability to mitigate reliably low RFI pulses that can affect radio astronomy observations.

It has been also shown that the system uses limited hardware resources, making possible its integration in a radio-astronomical back-end.

We plan to further test the proposed system with real data obtained through a measurement campaign, or directly in real time in the site affected by impulsive RFI such as Radars.

5 Acronyms

The following acronyms are used in this report:

AWGN: Additive White Gaussian Noise. A basic and generally accepted model for thermal noise in communication channels, whose effect on the signal of interest, is a linear addition of white noise with a constant spectral density and a Gaussian distribution of amplitude.

FIFO: First In First Out. A buffer used to store data implemented as a queue, i.e. the first data to be to be added to the queue will be the first data to be removed.

FPGA: Field Programmable Gate Array. An integrated digital circuit whose functionality is programmable externally via software.

INR: Interference to Noise Ratio

ITU-R: International Telecommunications Union- Radiocommunication Sector

LFSR: Linear Feedback Shift Register. A shift register whose input bit is a linear function (e.g. the exclusive-or (XOR)) of some bits of the overall shift register value. An LFSR with a suitable feedback function can produce a pseudorandom sequence of bits.

RAS: Radio Astronomy Service

RFI: Radio frequency Interference

ROC: Receiver Operating Characteristic. A graphical plot of the sensitivity, or correct decision rate, vs. false alarm rate

STLA: Signal Tap Logic Analyzer. A tool provided by the Quartus software that captures and displays real time signal behaviour of an FPGA design.

References

[1] N. Niamsuwan, J. T. Johnson, and S. W. Ellingson (2005), *Examination of a simple pulse-blanking technique for radio frequency interference mitigation*, Radio Sci., 40, RS5S03

[2] S. W. Ellingson and G. A. Hampson, *Mitigation of Radar Interference in L-Band Radio Astronomy*, 2003 ApJS 147 167

[3] D. Ait-Allal, R. Weber, C. Dumez-Viou, I. Cognard, and G. Theureau *RFI Mitigation Implementation for Pulsar Radioastronomy*,18th European Signal Processing Conference (EUSIPCO-2010), Aalborg, Denmark, August 23-27, 2010

[4] *SCFIFO and DCFIFO Megafunctions* Altera User Guide September 2010

[5] *Levels of data loss to radio astronomy observations and percentage-of-time criteria resulting from degradation by interference for frequency bands allocated to the radio astronomy on a primary basis* Rec. ITU-R RA.1513-1 1 RECOMMENDATION ITU-R RA.1513-1

Contents